HEAT TRANSFER FROM A PULSED LAMINAR IMPINGING JET

Hee Joo Poh* and Kurichi Kumar
Fluid Dynamics Division
Institute of High Performance Computing, 1 Science Park Road, #01-01 The Capricorn, Singapore 117528

Arun S. Mujumdar
Department of Mechanical Engineering, National University of Singapore,
9 Engineering Drive 1, Singapore 117576
*Corresponding Author. E-mail: pohhj@ihpc.a-star.edu.sg

ABSTRACT

A numerical investigation has been performed to study the effect of flow pulsations on time averaged Nusselt number under a laminar impinging jet. The parameters considered are: time-averaged jet Reynolds number ($100 \le Re \le 1000$), frequency of pulsation ($1 \le f \le 20$ Hz), and nozzle-to-target spacing ($4 \le H/d \le 9$). The combination of Re = 300, f = 5Hz and H/D = 9 was found to give the best heat transfer performance. Interestingly, it was found that the onset of separation at the wall jet region of pulsating impinging jet is associated with the point of constant Nusselt number during the oscillation cycle. Downstream of the separation point in the wall jet region, the Nusselt number waveform fluctuates out of phase with the inlet velocity. Within one oscillation, large vortices existing during the minimum velocity state are broken into two smaller vortices when the flow is accelerated to reach the maximum velocity, after which the two vortices merge again when the flow decelerates back to the minimum velocity.

Introduction

Due to its industrial importance in heating, cooling and drying applications, jet impingement heat transfer has been the topic of numerous investigations in recent years. However, most of the previous studies have focused on optimizing transport processes associated with steady jet impingement [1, 2]. Little work on pulsating impinging jet flows has been reported, probably because high convective heat transfer rates are readily attainable in using a turbulent impinging jet.

More recently, researchers have examined experimentally and numerically the potential for heat transfer enhancement via flow pulsations [3-13]. In pulsating flows, the flow situation is close to laminar during the acceleration phase, whereas turbulence can occur in the deceleration phase. This could lead to periodic transition from laminar to turbulent regime (and vice-versa), if the operating condition is near the critical Reynolds number [3]. As compared to steady impinging jet, the vortices in pulsating impinging jet are found to be larger and develop closer to the jet exit, thus resulting in the shortening and widening of the potential core of the jet and increased entrainment [4]. This would widen the high heat transfer region around stagnation zone. Mladin and Zumbrunnen [5] revealed that over one oscillation cycle in a planar pulsating impinging jet, the highest fluctuations of ensemble-averaged Nusselt number occurred at the mid-plane and approximately five (5) nozzle width downstream, while the smallest fluctuation was at one nozzle width downstream, attributed to significant fluid acceleration and damped turbulence effect there.

Some investigators have reported a marginal beneficial effect of pulsation [6 7], while others have claimed reported significant enhancement in heat transfer[5,8,9,10], because of either the interaction of large scale structures with the boundary layer (periodic formation of vortices structures generated in the shear layer impinging on the heated surface), or because of the secondary flow structures (vortex rings). However, some investigations involving jet pulsations show no enhancement or even deterioration of heat transfer due to pulsation[11,12], because the pulsation energy in these studies affects mainly the large scales of the flow and not the small structures which can enhance mixing, or because of the nonlinear dynamic responses of the hydrodynamic and thermal boundary layers. The sinusoidal variations of the incident jet velocity can induce non-sinusoidal responses in the instantaneous heat transfer coefficient even in the absence of incident vortex structures. In fact, the unsteady characteristics of impinging heat transfer are not yet fully understood, and therefore, the present work was conducted with the intention to resolve some of these issues via numerical simulations. The objective of this study is to investigate the effect of flow pulsations on time-averaged Nusselt number under axi-symmetric semi-confined laminar impinging water jets.

Conservation Equations

The pulsated impinging jet heat transfer problem is numerically computed with the commercial finite volume CFD code FLUENT 6.0, which solves the time-averaged Navier-Stokes and energy equations subject to specified boundary conditions on a given physical domain.

The equations for unsteady 2-D incompressible laminar flow one written as follows.

Conservation of mass

$$\frac{\partial}{\partial x}(\rho u)+\frac{1}{r}\frac{\partial}{\partial r}(\rho r v)=0 \tag{1}$$

Conservation of linear momentum

For x-momentum

$$\frac{\partial}{\partial x}(\rho u)+\frac{1}{r}\frac{\partial}{\partial x}(\rho uru)+\frac{1}{r}\frac{\partial}{\partial r}(\rho vru)=-\frac{\partial p}{\partial x}+\frac{\mu}{r}\frac{\partial}{\partial x}\left(r\frac{\partial u}{\partial x}\right)+\frac{\mu}{r}\frac{\partial}{\partial r}\left(r\frac{\partial u}{\partial r}\right) \qquad (2)$$

And for r-momentum

$$\frac{\partial}{\partial x}(\rho v)+\frac{1}{r}\frac{\partial}{\partial x}(\rho urv)+\frac{1}{r}\frac{\partial}{\partial r}(\rho vrv)=-\frac{\partial p}{\partial r}-\frac{uv}{r^2}+\frac{\mu}{r}\frac{\partial}{\partial x}\left(r\frac{\partial v}{\partial x}\right)+\frac{\mu}{r}\frac{\partial}{\partial r}\left(r\frac{\partial v}{\partial r}\right) \qquad (3)$$

Energy conservation

$$\frac{\partial}{\partial t}(\rho c_p T)+\frac{1}{r}\frac{\partial}{\partial x}\left[ur(\rho c_p T+p)\right]+\frac{1}{r}\frac{\partial}{\partial r}\left[vr(\rho c_p T+p)\right]=\frac{c_p\mu}{\Pr r}\frac{\partial}{\partial x}\left(r\frac{\partial T}{\partial x}\right)+\frac{c_p\mu}{\Pr r}\frac{\partial}{\partial r}\left(r\frac{\partial T}{\partial r}\right) \qquad (4)$$

The water jet of circular cross section and the fluid has constant physical properties such as density, specific heat and thermal conductivity. Hence, the geometric boundaries and physical conditions are symmetric about the axis of the jet. Gravitational effect is included. The axi-symmetric domain is shown in Figure 1. Only half of the domain is considered for the computations.

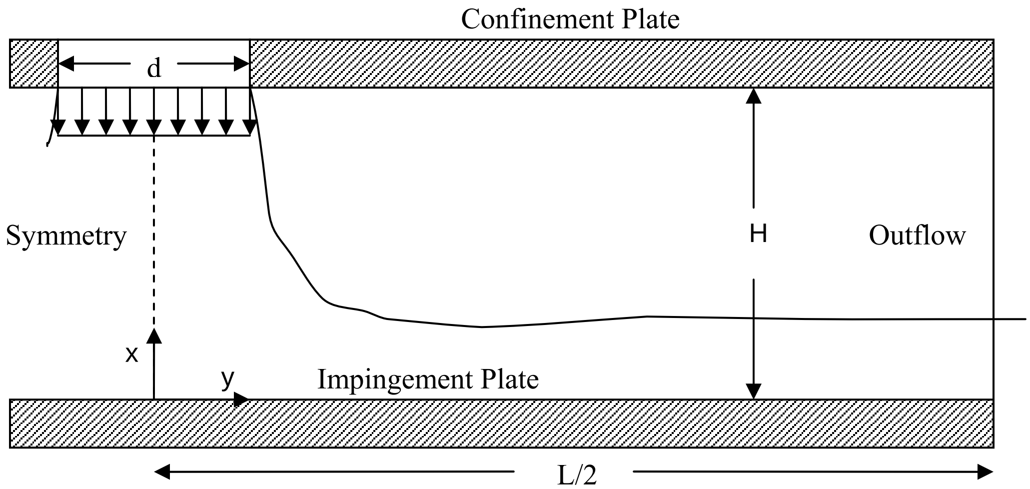

FIG. 1
Computational Domain

Boundary and Initial Conditions

A sinusoidally pulsating flat velocity profile is the boundary condition applied at the inlet of the domain. The waveform can be described by

$$u_{jet}=u_{avg}+u_{amp}\sin(2\pi ft) \quad , \qquad (5)$$

where $u_{avg} > u_{amp}$. The jet inlet temperature is constant and similar to atmospheric temperature (i.e. $T=T_{\infty}$). The boundary condition at the outflow is imposed with constant atmospheric pressure and temperature. $P_{outlet}=p_{\infty}$, $T_{outlet}=T_{\infty}$. No-slip condition with constant heat flux is imposed at the wall boundaries. The initial conditions (t = 0) throughout the computational domain are described as: u=v=0, $p=p_{\infty}$, $T=T_{\infty}$.

Results & Discussion

Figure 2 shows the predicted variation of the local impingement Nusselt number with time at various radial locations for f = 1Hz, H/D = 5, and at four different jet Reynolds numbers.

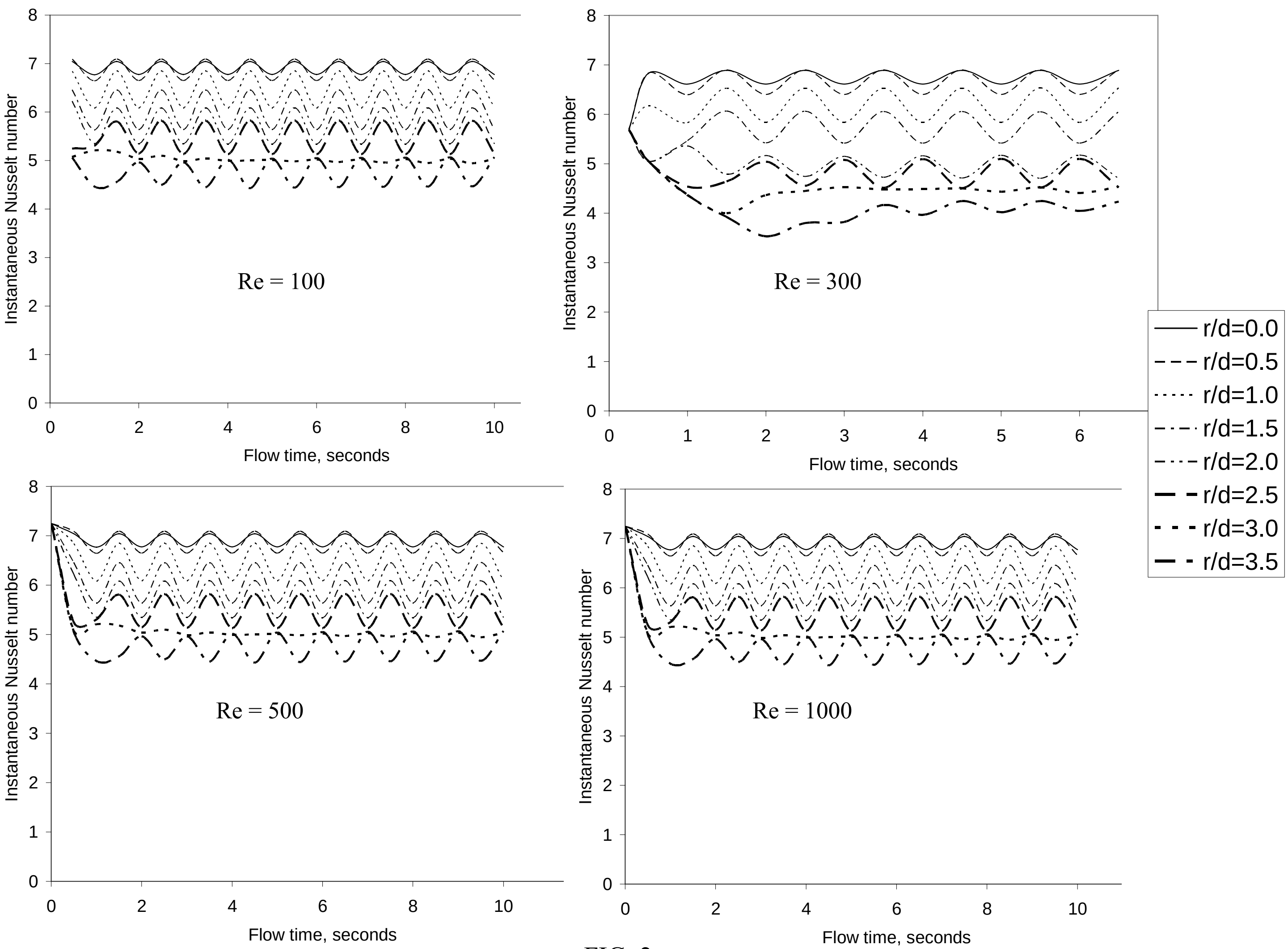

FIG. 2

Variation of Local Nusselt number with flow time for four Reynolds number at f = 1Hz, H/D = 5

From the above figure, it is noted that there is no improvement in heat transfer as the Reynolds number increases from 100 to 1000 in the laminar pulsating impinging jet. At lower Reynolds number, more damping was observed, attributed to the higher contribution of the viscous effect, whereas at a higher Reynolds number, the inertia effect is higher making the flow to follow the sinusodial profile more readily. Fluctuation in the local Nusselt number increases with radial distance from the stagnation point, but an exception occurs at r/d = 3. At r/d = 3, the Nusselt number remains almost constant during the oscillation cycle. This is attributed to existence of vortices above that location, which tend to suppress the flow acceleration and deceleration phenomena during the oscillation (c.f. Fig. 3). As the fluid moves radially outwards again, it starts to separate from the impingement wall, and causes the point downstream (r/d = 3.5) to be influenced by the flow oscillation again. Therefore, the point of constant Nusselt number can be regarded as the point of onset of separation. Another interesting observation is that beyond the separation point (r/d = 3), e.g. at r/d = 3.5, the Nusselt number waveform fluctuates out of phase with the inlet profile.

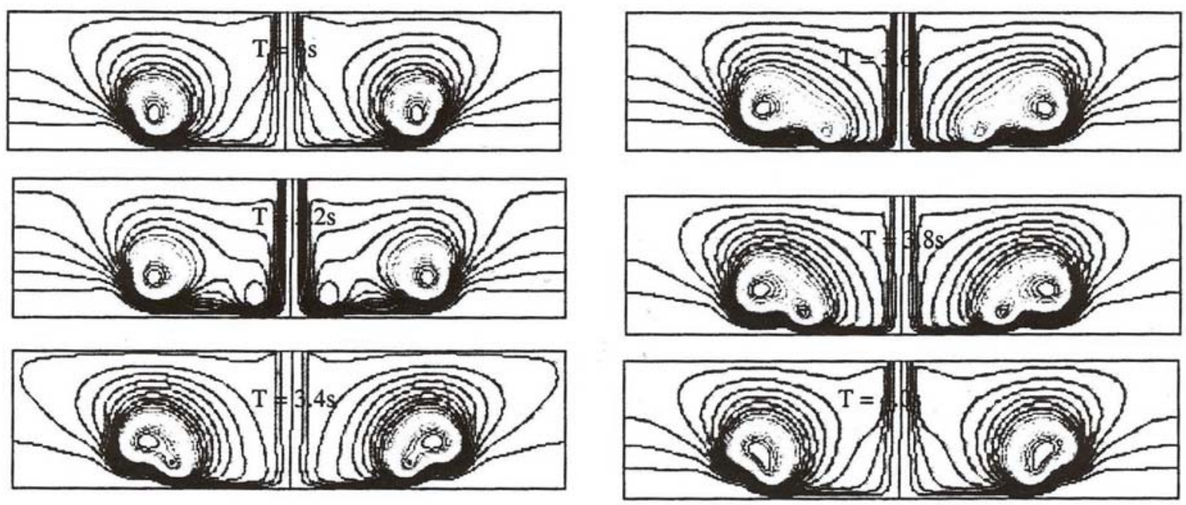

FIG. 3
Velocity Stream Functions contours during one complete oscillation cycle

From Figure 3, it can also be seen that the large vortices existing during the minimum velocity state (t = 3s) are broken into two smaller vortices when the flow is accelerated sinusodially to arrive at the maximum velocity (t = 3.6s), after which the two vortices merge again when the flow is decelerated back to the minimum velocity (t = 4s).

Figure 4 shows the variation local Nusselt with time at various radial locations for Re = 500, H/D = 5, at four different frequency of pulsation, *f*.

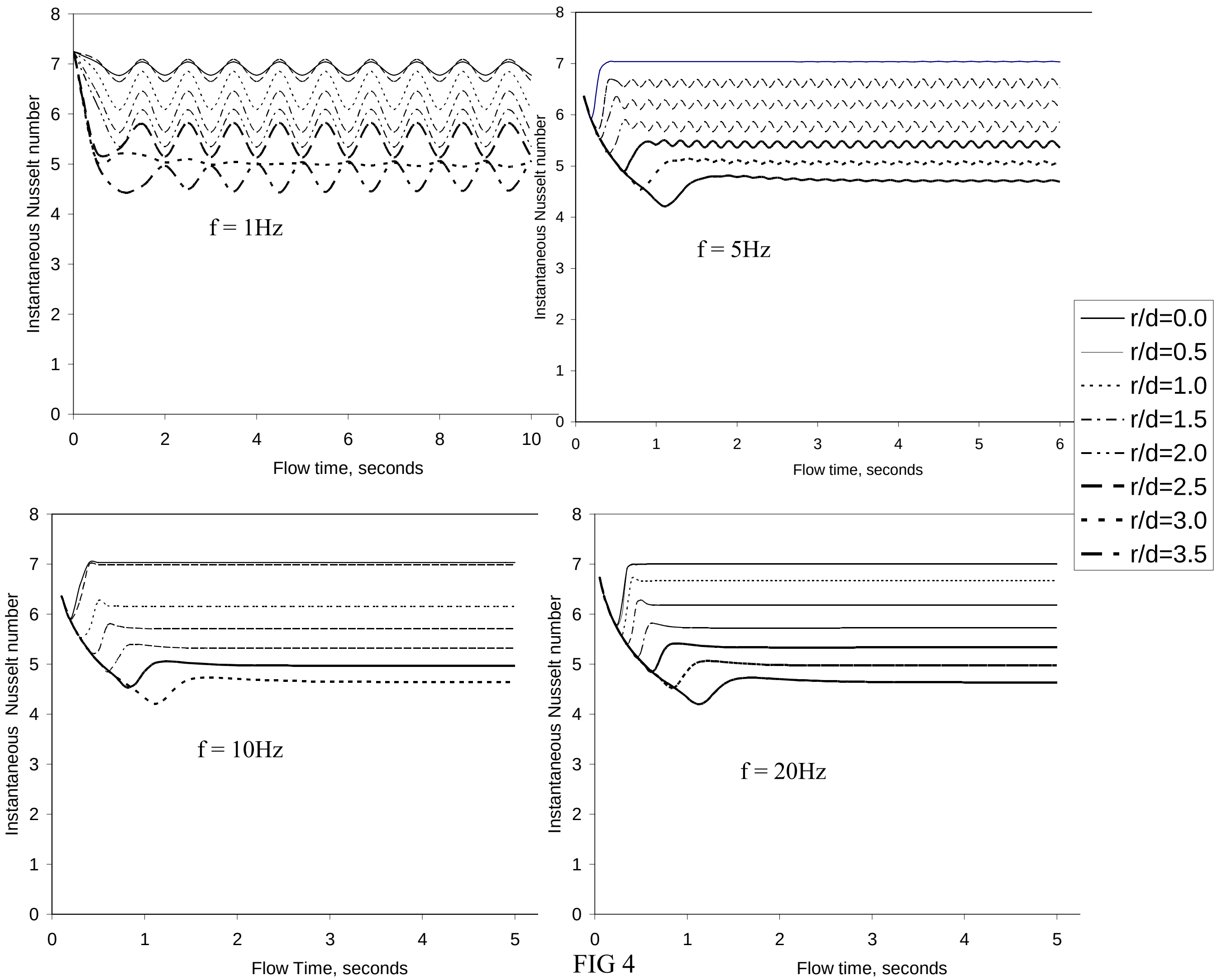

FIG 4

Variation of local Nusselt number with time at four different frequencies ; Re = 500, H/D = 5

The above figure shows that the amplitude of the Nusselt number fluctuations decreases with increasing frequency. No fluctuations in the waveform occur when $f = 20$Hz.

The time-averaged Nusselt number is defined as follows

$$Nu_{av,T} = \frac{1}{T_{pulse}} \int_{t=t_1}^{t_1+T_{pulse}} Nu_{av}\, dt \qquad (6)$$

Fig. 5a, b and c show the variation of time-averaged Nusselt number due to the effect of Reynolds number, frequency and nozzle-to-plate distance, respectively.

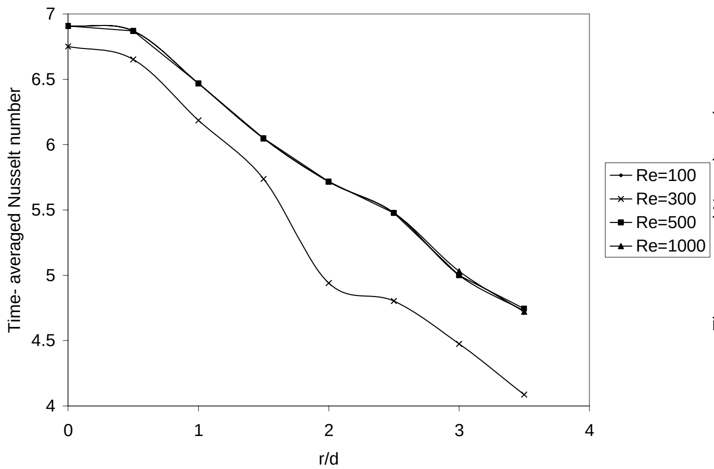

(a) Effect of Reynolds number

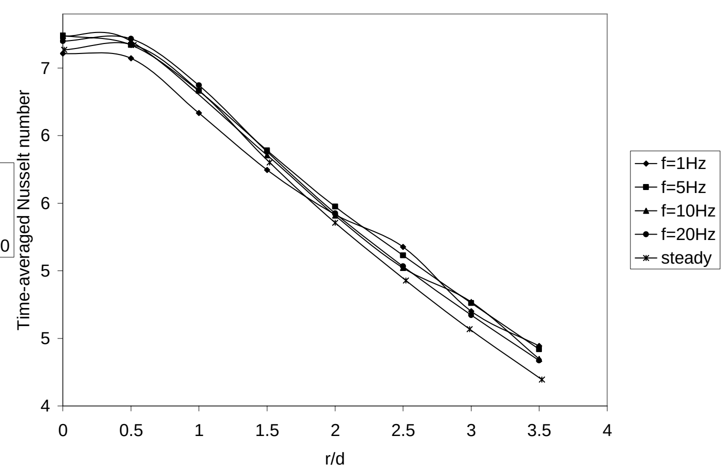

(b) Effect of frequency

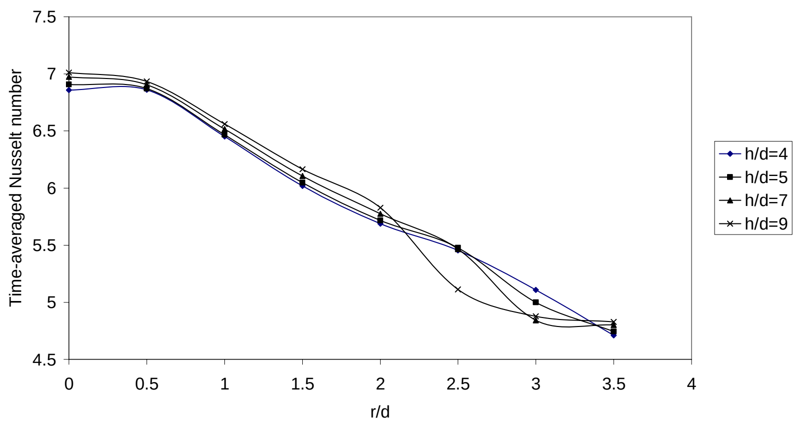

(c) Effect of nozzle-to-plate distance

FIG. 5
Effects on time-averaged Nusselt number due to various parameters

Fig. 5(a) shows that the time-averaged Nusselt numbers for all Reynolds number are within 17% of each other. However, it was noticed that Re = 300 gives the poorest heat transfer performance as compared to the lower Reynolds number of 100. This is an interesting phenomenon that is difficult to explain on physical grounds. There is a slight enhancement in the Nusselt number for all frequencies as compared to the equivalent steady jet (c.f. Fig. 5(b)). There is a periodic generation of vortices near the nozzle. These vortices enhance the mixing between the cold and the hot regions in some cases and increase the heat transfer. In the steady jet situation, there is neither a travelling vortex nor co-existence of multiple vortices but only one vortex core. The distance between the vortices is dependent on the frequency of the pulse. The Nusselt number is found to increase with increasing H/d (c.f. Fig. 5(c)), and this could be attributed to an increase in the free stream entrainment due to interaction between the jet and surrounding ambient.

Conclusions

From this study, it was found that the onset of separation at the wall jet region of pulsating impinging jet is associated with the point of constant Nusselt number during the oscillation cycle. This is attributed to the existence of vortices above that location, which tend to suppress the flow acceleration and deceleration phenomena during oscillation. Downstream of the separation point in the wall jet region, the Nusselt number waveform fluctuates out of phase with the inlet profile. Within one oscillation, large vortices exist during the minimum velocity state that would be broken into two smaller vortices when the flow is accelerated to reach at the maximum velocity, after which the two vortices will be merging again when the flow is decelerated back to the minimum velocity. It was also observed that among the various parameter combinations investigated (Reynolds number ($100 \leq Re \leq 1000$), frequency of pulsation ($1 \leq f \leq 20$ Hz), and nozzle-to-target spacing ($4 \leq H/d \leq 9$)), the combination of Re = 300, f = 5Hz and H/D = 9 gave the best heat transfer performance although the relative enhancement is marginal. Further studies, both computational and experimental are warranted to shed more light on the complex phenomena predicted.

Nomenclature

$A_N(\%)$	pulse amplitude $(=\frac{u_{\max}}{u_{amp}} x100)$
c_p	fluid specific heat (J kg^{-1} K^{-1})
d	diameter of circular nozzle (m)
f	frequency of the pulsating jet (Hz)
h	convective heat transfer coefficient (W m^{-2} K^{-1})
H	height of nozzle-to-wall spacing (m)
k	thermal conductivity (W m^{-1} K^{-1})
L	length of the wall (m)
L_n	nozzle plate thickness (m)
Nu	Nusselt number based on nozzle diameter $(=\frac{hd}{k}=\frac{q}{(T_w - T_\infty)}\frac{d}{k})$
p	pressure (N m^{-2})
Pr	fluid Prandtl number
q	wall heat flux (W m^{-2})

Re	Reynolds number based on nozzle diameter
t	time (s)
T	temperature (K)
u,v	velocities in x, r directions (m s^{-1})
u_{avg}	time-averaged velocity component of a pulsating jet (ms^{-1})
u_{amp}	periodic velocity component of a sine wave jet (m s^{-1})
u_{jet}	jet velocity (m s^{-1})
u_{rms}	root mean square value of the u_{amp} (m s^{-1})
U_m	centerline value of velocity
U_n	nozzle exit velocity
r,x	coordinate axes

<u>Greek Symbols</u>

μ	fluid dynamic viscosity (kg m^{-1} s^{-1})
ρ	fluid density (kg m^{-3})

<u>Subscripts</u>

avg	time-averaged value
amp	periodic value
r	radial
x	axial

<u>References</u>

1. B.W. Webb, and C.F. Ma, Single phase liquid jet impingement heat transfer, *Advances in Heat Transfer*, Vol. 26, pp. 105-217 (1995)

2. H. Martin, Heat and Mass Transfer between Impinging Gas Jets and Solid Surfaces, *Advances in Heat Transfer,* Vol. 13, pp. 1-60 (1977)

3. T.S. Zhao, and P. Cheng, Heat Transfer in Oscillatory Flow, *Annual Review of Heat Transfer,* Vol. 9, Begell House, New York (1998)

4. R.B. Farrington, and S.D. Claunch, Infrared Imaging of Large Amplitude, Low Frequency Disturbance on a Planar Jet, *AIAA Journal*, Vol. 32, pp. 317 – 323 (1994)

5. E. C. Mladin, and D. A. Zumbrunnen, Dependence of heat transfer to a pulsating stagnation flows on pulsation characteristics, *AIAA J. Thermophysics and Heat Transfer* Vol. 9 pp. 181-192, 1995

6. A. K. Chaniotis, D. Poulikakos, and Y. Ventkos, Dual Pulsating or Steady Slot Jet Cooling of a Constant Heat Flux Surface, *ASME Journal of Heat Transfer*, Vol 115 (Aug). pp. 575 – 586 (2003)

7. S.V.J. Narumanchi, C.H. Amon, and J.Y. Murthy, Influence of Pulsating Submerged Liquid Jets on Chip-Level Thermal Phenomena, *ASME Journal of Electronic Packaging*, Vol. 125 (Sep), pp.354-361 (2003)

8. E. C. Mladin, and D. A. Zumbrunnen, Local convective heat transfer to submerged pulsating jets", *Int. J. Heat Mass Transfer* 40 (14), pp. 3305-3321 (1997)

9. E. C. Mladin, and D. A. Zumbrunnen, , Alterations to coherent flow structures and heat transfer due to pulsations in an impinging air jet, *Int. J. Thermal Science* Vol. 39, pp. 236-248 (2000)

10. D. J. Sailor, D. J. Rohli, and Qianli Fu, Effect of variable duty cycle flow pulsations on heat transfer enhancement for an impinging air jet, *International Journal of Heat and Fluid Flow*, Vol.20, Issue 6 pp. 574-580 (1999)

11. L.F.A. Azevedo, B.W. Webb, and M. Queiroz, Pulsed Air Jet Impingement Heat Transfer, *Experimental Thermal & Fluid Science*, Vol. 8 (3), pp. 206-213 (1994)

12. H.S. Sherrif, and D.A. Zumbrunnen, Effect of flow pulsations on the cooling effectiveness of an impinging jet, *ASME Journal of Heat Transfer,* Vol. 116(Nov), pp. 886-895 (1994)

13. D.A. Zumbrunnen, and M. Aziz, Convective Heat Transfer Enhancement Due to Intermittency in an Impinging Jet, *ASME Juornal of Heat Transfer,* Vol 115 (Feb). pp. 91-98 (1993)